Social contagions on weighted networks

Yu-Xiao Zhu,[1,2,3] Wei Wang,[3,4] Ming Tang,[5,3,4,*] and Yong-Yeol Ahn[6,†]
[1]*School of Management, Guangdong University of Technology, Guangzhou 510520, China*
[2]*School of Big Data and Strategy, Guangdong University of Technology, Guangzhou 510520, China*
[3]*Web Sciences Center, University of Electronic Science and Technology of China, Chengdu 611731, China*
[4]*Big Data Research Center, University of Electronic Science and Technology of China, Chengdu 611731, China*
[5]*School of Information Science and Technology, East China Normal University, Shanghai 200241, China*
[6]*School of Informatics and Computing, Indiana University, Bloomington, Indiana 47408, USA*
(Received 7 April 2016; revised manuscript received 10 May 2017; published 5 July 2017)

We investigate critical behaviors of a social contagion model on weighted networks. An edge-weight compartmental approach is applied to analyze the weighted social contagion on strongly heterogenous networks with skewed degree and weight distributions. We find that degree heterogeneity cannot only alter the nature of contagion transition from discontinuous to continuous but also can enhance or hamper the size of adoption, depending on the unit transmission probability. We also show that the heterogeneity of weight distribution always hinders social contagions, and does not alter the transition type.

DOI: 10.1103/PhysRevE.96.012306

I. INTRODUCTION

Network provides a useful analytical framework for studying a wide array of social phenomena, since the network of people—social networks—plays a critical role in many social phenomena [1–6]. Although the edges in social networks—social relationships—are often modeled as binary, it is more realistic to consider *weighted* edges because the strength of social relationships greatly varies in reality [7]. A number of proxies has been used to capture the strength of social relationships. For example, the number of papers that two scientists have coauthored was used to capture the strength of the collaboration [7,8]; the duration of calls—the amount of conversation—between two people is used to measure how close they are [9]. Thus it is important to ask how the distribution of weights, along with degree distribution, affects various dynamics on networks.

Spreading processes, such as epidemic spreading [2,10–12], diffusion of innovations [13–15], and diffusion of rumors [16–18], are fundamental dynamics on social networks. Recent studies have shown that there exist two important classes of contagions: simple and complex. Simple contagions (e.g., epidemic models such as the SIS model [19] and SIR model [20]) refer the processes where contagions spread independently, while complex contagions (e.g., linear threshold model [21,22]) refer the processes that are affected by *social reinforcement*, where more exposures can drastically increase the adoption probability [15,22–25].

Previous studies, focused mainly on simple contagions, have revealed that strong heterogeneity in the degree and weight distributions not only is ubiquitous [2,7,26], but also fundamentally affects the nature of spreading phenomena [1,19,27–29]. For instance, small-world random networks with a degree distribution decaying slower than an exponential have a vanishing epidemic threshold in the thermodynamic limit [30]. The inhomogeneity of weight distribution can also significantly affect the epidemic threshold, epidemic prevalence, and spreading velocity [27,31–34]. Although many interesting properties of complex contagions have been uncovered recently [23,35–37], it is not fully understood how degree and weight heterogeneity affect the dynamics of complex contagions. Building on recent progress in complex contagions [15,22,38,39], here we introduce a weighted complex contagion model and investigate the effect of degree and weight heterogeneity on the dynamics of complex contagion.

We find that (i) increasing heterogeneity of degree distribution changes the nature of the phase transition from discontinuous to continuous; (ii) degree heterogeneity plays two opposite roles depending on the unit transmission probability: it enhances the spreading when the unit transmission probability is small while hinders the spreading when the unit transmission probability is large; and (iii) the weight heterogeneity suppresses the contagion while not altering the transition type. To analyze the dynamics of complex contagions on weighted networks, we use an edge-weight compartmental approach, which provides accurate results.

II. WEIGHTED COMPLEX CONTAGION MODEL AND NETWORK

We first introduce a complex contagion model that takes weighted edges into account. Our model builds on a simple, generalized non-Markovian contagion model that can describe both simple and complex contagions [15,40,41]. In particular, an individual can be in one of three possible states: *susceptible* (S), *adopted* (A), or *recovered* (R). Each individual has a state of integer awareness value $m \in [0,T]$ which denotes the exact received pieces of cumulative information. An individual adopts and *begins to transmit* the behavior or information (contagion) when its awareness value reaches T. Individuals with $m < T$ do not affect the others. Here we add a weight-based transmission rule—individuals transmit the contagion preferably to its closer neighbors with the following probability:

$$\lambda_{w_{i,j}} = 1 - (1-\beta)^{w_{i,j}}, \tag{1}$$

*tangminghan007@gmail.com
†yyahn@indiana.edu

where $w_{i,j}$ is positive real integer, which denotes the weight of the connection between individual i and j, and β is the unit transmission probability. Given β, $\lambda_{w_{i,j}}$ monotonically increases with $w_{i,j}$, i.e., individuals are more likely to transmit the contagion to more strongly connected neighbors. Also note that the probabilities are indeed rates and defined per time. When successful, the awareness value of the neighbor will increase by one. Edges that have transmitted the contagion successfully will never transmit the same information again. Also, each adopted individual may become recovered with probability γ, considering the fact that people may lose interest in the contagion after a while and will not spread it any more (in this paper, we set $\gamma = 1$ unless noted, so everyone is active for only one step). The individuals will remain in recovered state for all subsequent times once recovered. Note that, each individual can remember the cumulative pieces of non-redundant that received from his/her neighbors in our model, which makes the contagion processes become non-Markovian. This is different with SIR and SEIS models [20,42], in which whether the susceptible individual gets adopted only depends on the neighbors current states. Also note that we applied the synchronous updating method to renew the states of individuals. In this case, the time evolves discretely.

In our networks, we initially select a small fraction of nodes randomly and designate them as *seeds* by setting their awareness to be T. We set the awareness of the remaining nodes to be 0 and let them be at the susceptible state. In each step, all adopted nodes will interact with all of their susceptible neighbors and transmit the contagion to them with the probability defined above. At the same time, all adopted nodes will recover with probability 1. The spreading process stops when there are no adopted nodes, the final adoption size is equal to the final density of recovered nodes.

For simplicity, we assume uncorrelated random graphs specified by two distributions: degree and weight. We realize such networks by generalizing the configuration model [27,43]. Consider one network with N nodes and M edges. We first create a graph using the classical configuration model, where the degree distribution follows $p(k) \sim k^{-\alpha_k}$ $(3 \leqslant k_i \leqslant \sqrt{N})$, then distribute weights that are sampled from $g(w) \sim w^{-\alpha_w}$ randomly $(w_{\max} \sim N^{\frac{1}{\alpha_w - 1}})$. α_k (α_w) controls the heterogeneity of the degree (weight) distribution [2], heterogenous distribution is commonly used to describe highly skewed distribution. Following previous studies [27,34], we assume integer weight values as it makes our approach more tractable.

III. THEORETICAL APPROACH AND NUMERICAL SIMULATION

A. Edge-weight compartmental approach

One of the most widely used approaches to study network dynamics—heterogeneous mean-field theory (HMF) [20,44]—separates nodes into each degree bucket while treating all edges equally. While it provides an excellent way to handle strong degree heterogeneity, it overlooks edge weight heterogeneity. As a result, the approach exhibits a limitation in dealing with networks with strong weight heterogeneity [45]. Our edge-weight compartmental approach treats each (integer) weight values separately and provides a better way to study networks with strong weight heterogeneity [27,46–48].

We use variables $S(t)$, $A(t)$, and $R(t)$ to denote densities of the susceptible, adopted, and recovered nodes at time t. Let us consider a randomly selected susceptible node u with awareness value m. Node u will remain susceptible as long as $m < T$ and will become adopted once T of its neighbors have transmitted the contagion successfully to u since multiple transmission through an edge is forbidden. As edge weights are assigned randomly, the probability that u is not informed by a neighbor v by time t can be denoted by

$$\theta(t) = \sum_{w} g(w)\theta_w(t), \tag{2}$$

where $\theta_w(t)$ denotes the probability that u is not informed by an edge with weight w by time t. If u's degree is k, the probability that the node was not one of the seeds and has been exposed to the contagion for m times by time t is

$$\phi_m(k,t) = (1-\rho_0)\binom{k}{m}[\theta(t)]^{k-m}[1-\theta(t)]^m, \tag{3}$$

where A_0 denotes the fraction of seeds. Clearly, the probability that the k-degree node was not one of the seeds and still did not adopt the contagion by time t is

$$\phi(k,t) = \sum_{m=0}^{T-1} \phi_m(k,t). \tag{4}$$

Thus the fraction of susceptible nodes (the probability that a randomly selected node is susceptible) at time t is

$$S(t) = \sum_{k=0} p(k)\phi(k,t). \tag{5}$$

Now, let us examine $\theta_w(t)$ in Eq. (2), $\theta_w(t)$ can be broken down into

$$\theta_w(t) = \xi_w^S(t) + \xi_w^A(t) + \xi_w^R(t), \tag{6}$$

where $\xi_w^X(t)$ denote the probability that a neighbor in the state $X \in \{\mathrm{S},\mathrm{A},\mathrm{R}\}$ has not transmitted the contagion to u through an edge with weight w by time t. Once we derive $\xi_w^X(t)$s, we can get the density of susceptible nodes at time t by substituting them into Eqs. (2)–(5).

Only neighbors that are in an adopted state can inform u. So first let us calculate the probability that the neighbor remains to be susceptible by t. As we assume no correlation between the degrees of nodes and its neighbors exist in uncorrelated networks, the probability that a random neighbor of u has degree k is $kp(k)/\langle k\rangle$, where $\langle k\rangle$ is the mean degree of the network. With mean-field approximation, $\xi_w^S(t)$ is simply the probability that one of its neighbors remains in the susceptible state by time t, which is given by

$$\xi_w^S(t) = \frac{\sum_k kp(k)\phi(k-1,t)}{\langle k\rangle}. \tag{7}$$

Note that, as we already know, u is in a susceptible state at this time, so the probability that this k-degree neighbor still did not adopt the behavior by time t is $\phi(k-1,t)$.

Calculating $\xi_w^R(t)$ requires considering two consecutive events: first, an adopted neighbor has not transmitted the

contagion to node u via their edge with weight w with probability $1-\lambda_w$; second, the adopted neighbor has been recovered, with probability γ. Combining these two events, we have

$$\frac{d\xi_w^R(t)}{dt} = \gamma[1-\lambda_w]\xi_w^A(t). \tag{8}$$

If this adopted neighbor transmits the contagion via an edge with weight w, the rate of flow from $\theta_w(t)$ to $1-\theta_w(t)$ will be $\lambda(w)\xi_w^A(t)$, which means

$$\frac{d\theta_w(t)}{dt} = -\lambda_w\xi_w^A(t) \tag{9}$$

and

$$\frac{d(1-\theta_w(t))}{dt} = \lambda_w\xi_w^A(t). \tag{10}$$

By combining Eqs. (8) and (10), one obtains

$$\xi_w^R = \frac{\gamma[1-\theta_w(t)][1-\lambda_w]}{\lambda_w}. \tag{11}$$

Substituting Eqs. (7) and (11) into Eq. (6), we yield the following relation:

$$\xi_w^A(t) = \theta_w(t) - \frac{\sum_k kp(k)\phi(k-1,t)}{\langle k\rangle} - \frac{\gamma[1-\theta_w(t)][1-\lambda_w]}{\lambda_w}. \tag{12}$$

By plugging this into Eq. (9), we obtain

$$\frac{d\theta_w(t)}{dt} = \frac{\lambda_w\sum_k kp(k)\phi(k-1,t)}{\langle k\rangle} - (1-\gamma)\lambda_w\theta_w(t) + \gamma[1-\lambda_w-\theta_w(t)]. \tag{13}$$

From Eq. (13), the probability $\theta_w(t)$ can be computed. The density associated with each distinct state is given by

$$\frac{dR(t)}{dt} = \gamma A(t),$$
$$S(t) = \sum_{k=0} p(k)\phi(k,t),$$
$$A(t) = 1 - R(t) - S(t). \tag{14}$$

From Eqs. (13) and (14), one can find that around $O(w_{\max})$ equations are required in our edge-weight compartmental approach. By setting $t\to\infty$ and $d\theta_w(t)/dt = 0$ in Eq. (13), we get the probability of one edge with weight w that did not propagate the contagion in the whole contagion process:

$$\theta_w(\infty) = \frac{\gamma[1-\lambda_w] + \frac{\lambda_w\sum_k kp(k)\phi(k-1,\infty)}{\langle k\rangle}}{(1-\gamma)\lambda_w+\gamma}. \tag{15}$$

$\theta_w(t)$ decreases with t and thus if more than one stable fixed point exists in Eq. (15), only the maximum one is physically meaningful [40,48]. Substituting $\theta_w(\infty)$ into Eqs. (2)–(5), we can calculate the value of $S(\infty)$, and then final adoption size $R(\infty)$ can be obtained. The number of roots in Eq. (15) is either one or three. If Eq. (15) has only one root, $R(\infty)$ increases continuously with β, if Eq. (15) has three roots, a saddle-node bifurcation will occur, which leads to a discontinuous change in $R(\infty)$ [49]. The nontrivial solution corresponds to the point at which the equation

$$f(\theta(\infty)) = \sum_w g(w)\frac{\gamma[1-\lambda_w] + \frac{\lambda_w\sum_k kp(k)\phi(k-1,\infty)}{\langle k\rangle}}{(1-\gamma)\lambda_w+\gamma} - \theta(\infty) \tag{16}$$

is tangent to horizontal axis at the critical value of $\theta_c(\infty)$, in which $\theta_c(\infty)$ means the critical probability that the information is not transmitted to u via an edge at the critical transmission probability when $t\to\infty$. We obtain the critical condition of contagion by

$$\frac{df(\theta(\infty))}{d\theta(\infty)}|_{\theta_c(\infty)} = 0. \tag{17}$$

Plugging $\theta_c(\infty)$ into Eq. (2) provides us with the critical probability β_c.

B. Simulation results

We report results of analytical solutions along with numerical simulations. We consider networks with power-law degree and weight distributions: $p(k)\sim k^{-\alpha_k}$ and $g(w)\sim w^{-\alpha_w}$. We use $A_0 = 0.1$ across the article but the results are robust with a range of A_0. Also we use, for each parameter combination, 50 network realizations, on each of which we run 100 independent simulations.

Figure 1 illustrates the time evolutions of susceptible (S), adopted (A), and recovered (R) nodes. Naturally, it displays a very similar dynamics as with the SIR model. Our analytical results (lines) agree well with simulation results (symbols). In Fig. 2(a), we show the final adoption size $[R(\infty)]$ in relationship with unit transmission probability (β) for networks with different degree and weight distributions along with the analytical results (shown in black line, which match well with the simulation results). Now, let us focus on the influence of heterogeneous degree distribution on social contagion processes from two perspectives: the transition type

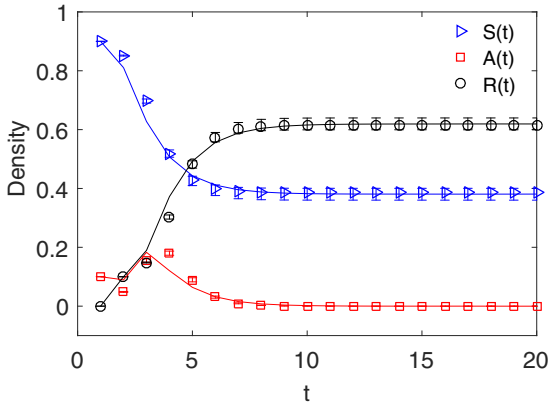

FIG. 1. Time evolutions of densities of nodes in different states, denoted by $S(t)$ (blue triangles), $A(t)$ (red squares), and $R(t)$ (black circles), respectively. Analytical results are plotted in lines, which match well with simulation results (symbols). The parameters for the simulations are $N = 10{,}000$, $\langle k\rangle = 10$, $\langle w\rangle = 8$, $\alpha_k = 2.1$, $\alpha_w = 2.4$, $\beta = 0.18$, $A_0 = 0.1$, and $T = 3$.

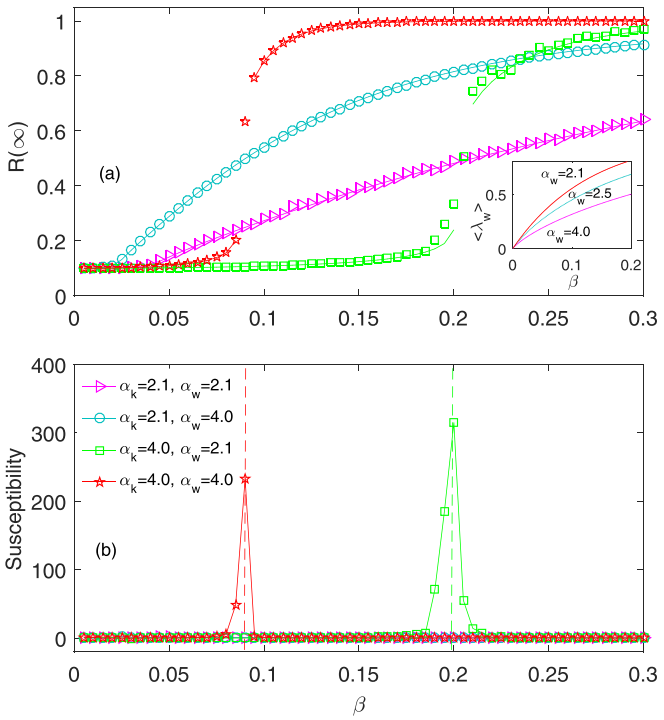

FIG. 2. Final states of complex contagion dynamics on weighted networks. (a) Final adoption size $[R(\infty)]$ versus the unit transmission probability (β) on different networks with tunable parameters. The inset shows the numerical solutions of mean transmission rate $\langle\lambda_w\rangle$ as function of β for three different values of α_w (i.e., 2.1, 2.5, and 4.0). (b) Susceptibility versus the β on different networks with tunable parameters. The parameters for all the simulations are $N = 10{,}000$, $\langle k\rangle = 10$, $\langle w\rangle = 8$, $A_0 = 0.1$, and $T = 3$.

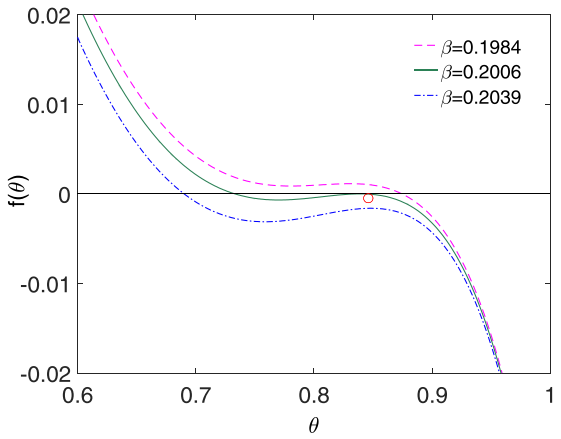

FIG. 3. Illustration of graphical solutions of Eq. (15). The black solid line is the horizontal axis and the red circle denotes the tangent point. The parameters for the simulations are $N = 10{,}000$, $\langle k\rangle = 10$, $\langle w\rangle = 8$, $\alpha_k = 4.0$, $\alpha_w = 2.1$, $A_0 = 0.1$, and $T = 3$.

of $R(\infty)$ with β and the final adoption size. We summarize our results as follows.

First, the degree exponent determines the discontinuity of the transition as shown in a previous work [48]. Figure 2(a) shows that $R(\infty)$ increases continuously with β with heterogeneous degree distribution (e.g., $\alpha_k = 2.1$), while exhibiting a discontinuous transition when $\alpha_k = 4.0$. The results of bifurcation analysis on Eq. (15) show that there exists one critical degree exponent $\alpha_k^c \approx 4.0$, below (above) which $R(\infty)$ versus β is continuous (discontinuous). For networks with $\alpha_k = 4.0$, the value of β_c can be obtained from Eq. (15) using bifurcation theory [49]. Analytical calculations show that for Eq. (15), the number of roots in Eq. (15) is either one or three (see Fig. 3). If Eq. (15) has only one root, $R(\infty)$ increases continuously with β; if Eq. (15) has three roots, a saddle-node bifurcation occurs [49]. As shown in Fig. 3, there is only one fixed point of Eq. (15) at a small value of β (e.g., $\beta = 0.1984$) and then three fixed points [in this case, only the maximum one is physically meaningful since $\theta(t)$ decreases with t] gradually emerge with the increasing of β. The tangent point that is marked as one red circle is the physically meaningful solution at the unit transmission probability β_c (e.g., $\beta = 0.2006$). For $\beta > \beta_c$ (e.g., $\beta = 0.2039$), the solution of Eq. (15) changes to a smaller solution abruptly, which leads to a discontinuous change in $R(\infty)$. We can demonstrate the type of dependence and obtain the value of β_c for other parameters through the similar measure.

We also explain this phenomena visually by showing susceptibility in Fig. 2(b), susceptibility [50] is defined as

$$\chi = N\frac{\langle R(\infty)^2\rangle - \langle R(\infty)\rangle^2}{\langle R(\infty)\rangle}. \tag{18}$$

Clearly, for results in Fig. 2(b), each phase transition corresponds to one peak of susceptibility. The critical value β_c can also be estimated by increasing the number of iterations [51] (only those interactions in which at least one newly adopted individual appears are taken into account). In Fig. 2(b), we show the estimated β_c with dashed lines, which correspond to the peaks of susceptibility. More details are shown in Fig. 4. As we expected, $R(\infty)$ for networks with heterogeneous degree distribution [Fig. 4(a)] shows a continuous change with the increasing of β while change discontinuously on networks with homogeneous degree distribution [Fig. 4(c)]. Analytical results shown in Fig. 4(b),(d) agree well with numerical results. The estimated values of β_c are labeled with a blue circle, along with the corresponding analytical critical results plotted with a blue line [shown in Figs. 4(d)].

Second, as a result of continuous-discontinuous transition, degree heterogeneity enhances the final adoption size at small β while hindering it at large β, which is consistent with that of the epidemic case [27]. For instance, when $\alpha_w = 2.1$, the final adoption size $[R(\infty)]$ for $\alpha_k = 2.1$ is greater than that of $\alpha_k = 4.0$ when $\beta < 0.2$, while the opposite situation is obtained when $\beta > 0.2$ [shown in Fig. 2(a)]. This result can be qualitatively explained as follows: social contagion propagates on complex networks in two stages due to the co-emergence of more hubs and a large amount of small-degree nodes with increasing heterogeneity of degree distribution. The hubs are more likely to become adopted early since more neighbors make them have a higher chance to reach the identical awareness threshold T and thus get adopted. On the contrary, small-degree nodes are less likely to become adopted due to the small number of neighbors. Given a network with

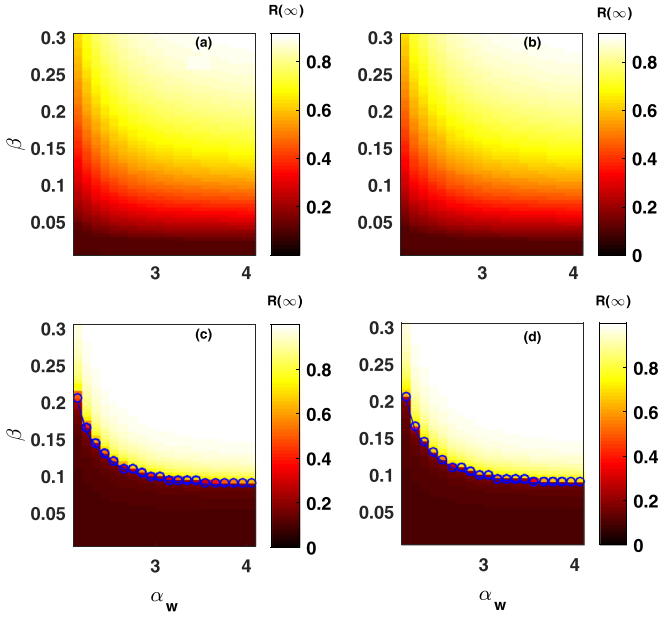

FIG. 4. The relationships between α_w, β, and $R(\infty)$ at a fixed α_k. (a) and (b) are results of numerical simulation and analytical method on networks with $\alpha_k = 2.1$, while (c) and (d) are those of $\alpha_k = 4.0$ respectively. The parameters for simulation are $N = 10{,}000$, $\langle k\rangle = 10$, $\langle w\rangle = 8$, $A_0 = 0.1$, and $T = 3$.

heterogeneous degree distribution, when unit transmission probability β is small, the existence of more hubs enhances the contagion and thus leads to greater $R(\infty)$ (promotion region); When β is large, the existence of a large amount of small-degree nodes will hinder the contagion, resulting in smaller $R(\infty)$ (suppression region). Figure 5 shows the whole

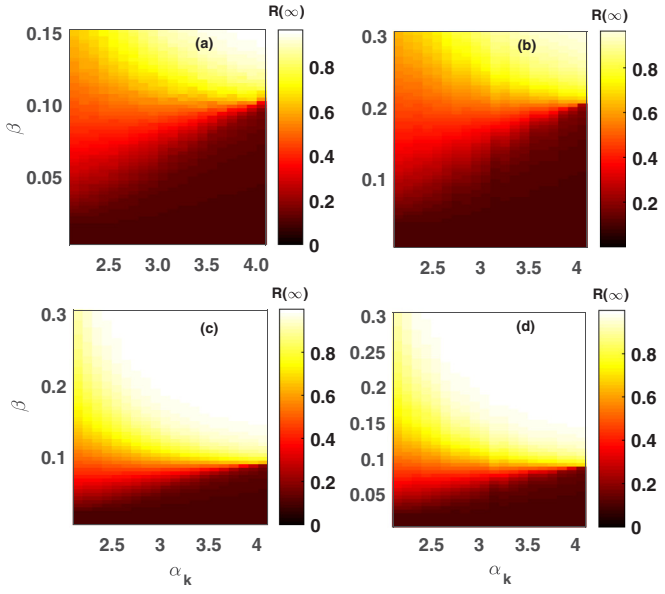

FIG. 5. The relationships between α_k, β, and $R(\infty)$ at a fixed α_w. (a) and (b) are results of numerical simulation and analytical method on networks with $\alpha_w = 2.1$, while (c) and (d) are those of $\alpha_w = 4.0$ respectively. The parameters for the simulations are $N = 10{,}000$, $\langle k\rangle = 10$, $\langle w\rangle = 8$, $A_0 = 0.1$, and $T = 3$.

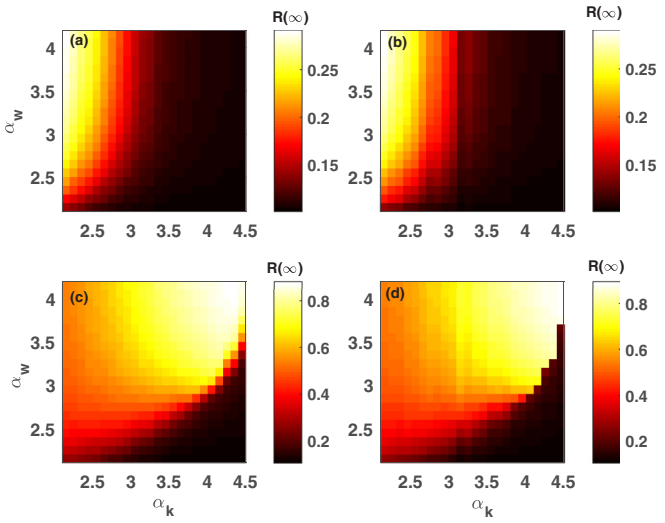

FIG. 6. The relationships between α_k, α_w, and $R(\infty)$ when the unit transmission probability β is fixed. (a) and (b) are results of numerical simulation and analytical method on the weighted contagion model with $\beta = 0.05$, while (c) and (d) are those of $\beta = 0.1$ respectively. The parameters for the simulations are $N = 10{,}000$, $\langle k\rangle = 10$, $\langle w\rangle = 8$, $A_0 = 0.1$, and $T = 3$.

picture of the relationship between α_k, β, and $R(\infty)$ when fixing α_w. Increasing the heterogeneity of degree distribution will enhance $R(\infty)$ at small β while hindering the adoption size at large β.

Let us address the influence of the heterogeneity of weight distribution on social contagion processes at a given α_k. The heterogeneity of weight distribution (smaller value of α_w) reduces final adoption size $R(\infty)$. For instance, if we fix α_k [Fig. 2(a)], $R(\infty)$ for $\alpha_w = 2.1$ is always smaller than that of $\alpha_w = 4.0$. This phenomenon can be explained as follows: when the average weight $\langle w\rangle$ is fixed, in the network with smaller α_w, most edges have lower weights and thus transmission probabilities, leading to a smaller mean transmission rate $\langle\lambda_w\rangle = \sum_w g(w)\lambda_w$ for a randomly selected edge. As shown in the inset of Fig. 2(a), $\langle\lambda_w\rangle$ of $\alpha_w = 2.1$ is smaller than that of $\alpha_w = 4.0$ with a given β. On the other hand, changing the weight distribution will not change the dependence behavior of $[R(\infty), \beta]$ with a given degree distribution, which is similar to the case of simple contagion models [27]. This finding can be verified from analytical perspective, varying the value of α_w will not change the number of roots in Eq. (15), thus will not affect whether saddle-node bifurcation occurs or not. The relationship between α_w and β when fixing α_k is shown in Fig. 4, which confirms our finding here.

Finally, Fig. 6 summarizes our results, showing that for a small value of transmission probability ($\beta = 0.05$), the existence of more hubs that can be easily informed thus enhances the contagion process (promotion region). While for a large value of transmission probability ($\beta = 0.1$), the existence of large-amount small-degree nodes that are difficult to be adopted will hinder the contagion process (suppression region). In addition, increasing the heterogeneity of weight distribution will always hinder $R(\infty)$. Figures 6(a),(c) and

6(b),(d) show the results of simulation and analytical methods, respectively, which match well with each other.

IV. CONCLUSIONS

In summary, we study the effect of heterogenous network structures on the diffusion of complex contagions. With decreasing heterogeneity of degree distribution, the dependence of the final adoption size on unit transmission probability changes from being continuous to discontinuous. We then show that the heterogeneity of degree distribution may have two opposite effects depending on the transmission probability: degree heterogeneity enhances complex contagions when β is small while hindering it when β is large. By contrast, the heterogeneity of weight distribution always reduces the final adoption size though does not change the dependence pattern of final adoption size on the unit transmission probability. In order to describe the non-Markovian characteristic and weight-based transmission rule by the edge-weight based compartmental theory, we made efforts from two aspects. On the one hand, in order to consider the non-Markovian characteristic, we first developed content of $\theta_w(t)$ to denote the probability that the individual u in the cavity state is not informed by an edge with weight w by time t, then introduced the memory into Eqs. (3) and (7). On the other hand, we let the α_k and α_w be heterogeneous to study the effects of heterogeneous structures. The edge-weight compartmental approach can predict the proposed model well.

Our findings offer insights to understand the influence of underlying network structures for weighed social contagions. Future work may investigate the nature of bifurcation, the cases where the adoption threshold of each individual varies with its degree, or a richer and correlated network structure is assumed.

ACKNOWLEDGMENTS

This work was partially supported by the National Natural Science Foundation of China (Grants No. 11105025, No. 11575041, No. 61433014, and No. 71571052) and Guangdong science and technology plan project (No. 15ZS0117). Y.Y.A. thanks Microsoft Research for MSR Faculty Fellowship.

[1] M. E. J. Newman, SIAM Rev. **45**, 167 (2003).
[2] R. Pastor-Satorras, C. Castellano, P. V. Mieghem, and A. Vespignani, Rev. Mod. Phys. **87**, 925 (2015).
[3] C. Castellano, S. Fortunato, and V. Loreto, Rev. Mod. Phys. **81**, 591 (2009).
[4] S. Boccaletti, V. Latora, Y. Moreno, M. Chavez, and D.-U. Hwang, Phys. Rep. **424**, 175 (2006).
[5] R. Cohen and S. Havlin, *Complex Networks: Structure, Robustness and Function* (Cambridge University Press, Cambridge, 2010).
[6] A.-L. Barabási, *Network Science* (Cambridge University Press, Cambridge, 2015).
[7] A. Barrat, M. Barthelemy, R. Pastor-Satorras, and A. Vespignani, Proc. Natl. Acad. Sci. USA **101**, 3747 (2004).
[8] M. E. J. Newman, Proc. Natl. Acad. Sci. USA **98**, 404 (2001).
[9] J.-P. Onnela, J. Saramäki, J. Hyvönen, G. Szabó, M. A. de Menezes, K. Kaski, A.-L. Barabási, and J. Kertész, New J. Phys. **9**, 179 (2007).
[10] M. E. J. Newman, *Networks: An Introduction* (Oxford University Press, Oxford, 2010).
[11] D. Easley and J. Kleinberg, *Networks, Crowds, and Markets: Reasoning About a Highly Connected World* (Cambridge University Press, Cambridge, 2010).
[12] C. Nowzari, V. M. Preciado, and G. J. Pappas, IEEE Control Syst. Mag. **36**, 26 (2016).
[13] E. M. Rogers, *Diffusion of Innovations* (Free Press, New York, USA, 2003).
[14] W. Goffman and V. A. Newill, Nature **204**, 225 (1964).
[15] P. L. Krapivsky, S. Redner, and D. Volovik, J. Stat. Mech. (2011) P12003.
[16] Y. Moreno, M. Nekovee, and A. F. Pacheco, Phys. Rev. E **69**, 066130 (2004).
[17] D. J. Daley and D. G. Kendall, Nature **204**, 1118 (1964).
[18] J.-J. Cheng, Y. Liu, B. Shen, and W.-G. Yuan, Eur. Phys. J. B **86**, 29 (2013).
[19] R. Pastor-Satorras and A. Vespignani, Phys. Rev. Lett. **86**, 3200 (2001).
[20] Y. Moreno, R. Pastor-Satorras, and A. Vespignani, Eur. Phys. J. B **26**, 521 (2002).
[21] M. Granovetter, Am. J. Sociol. **83**, 1420 (1978).
[22] D. J. Watts, Proc. Natl. Acad. Sci. USA **99**, 5766 (2002).
[23] D. Centola, Science **329**, 1194 (2010).
[24] L. Backstrom, D. Huttenlocher, J. Kleinberg, and X. Lan, in *Proceedings of the 12th ACM SIGKDD International Conference on Knowledge Discovery and Data Mining, Philadelphia, PA* (ACM, New York, 2006), pp. 44–54.
[25] J. C. Miller, J. Complex Netw. **4**, 201 (2016).
[26] R. Albert and A.-L. Barabási, Rev. Mod. Phys. **74**, 47 (2002).
[27] W. Wang, M. Tang, H. F. Zhang, H. Gao, Y. H. Do, and Z. H. Liu, Phys. Rev. E **90**, 042803 (2014).
[28] T. Gross and B. Blasius, J. R. Soc. Interface **5**, 259 (2008).
[29] P. Holme and J. Saramäki, Phys. Rep. **519**, 97 (2012).
[30] M. Boguñá, C. Castellano, and R. Pastor-Satorras, Phys. Rev. Lett. **111**, 068701 (2013).
[31] C. Kamp, M.-L. Mathieu, and S. Alizon, PLoS Comput. Biol. **9**, e1003352 (2013).
[32] P. Rattana, K. B. Blyuss, K. T. D. Eames, and I. Z. Kiss, Bull. Math. Biol. **75**, 466 (2013).
[33] G. Yan, T. Zhou, J. Wang, Z. Q. Fu, and B. H. Wang, Chin. Phys. Lett. **22**, 510 (2005).
[34] Z. M. Yang and T. Zhou, Phys. Rev. E **85**, 056106 (2012).
[35] J. P. Gleeson, Phys. Rev. E **77**, 046117 (2008).
[36] L. Weng, F. Menczer, and Y.-Y. Ahn, Sci. Rep. **3**, 02522 (2013).
[37] A. Nematzadeh, E. Ferrara, A. Flammini, and Y.-Y. Ahn, Phys. Rev. Lett. **113**, 088701 (2014).
[38] P. S. Dodds and D. J. Watts, Phys. Rev. Lett. **92**, 218701 (2004).
[39] T. C. Schelling, J. Math. Sociol. **1**, 143 (1971).
[40] W. Wang, M. Tang, P.-P. Shu, and Z. Wang, New J. Phys. **18**, 013029 (2015).

[41] W. Wang, P.-P. Shu, M. Tang, and Y.-C. Zhang, Chaos **25**, 103102 (2015).
[42] M. Fan, M. Y. Li, and K. Wang, Math. Biosci. **170**, 199 (2001).
[43] M. Catanzaro, M. Boguñá, and R. Pastor-Satorras, Phys. Rev. E **71**, 027103 (2005).
[44] C. Castellano and R. Pastor-Satorras, Phys. Rev. Lett. **96**, 038701 (2006).
[45] C. Buono, F. Vazquez, P. A. Macri, and L. A. Braunstein, Phys. Rev. E **88**, 022813 (2013).
[46] E. M. Volz, J. Math. Biol. **56**, 293 (2008).
[47] E. M. Volz, J. C. Miller, A. Galvani, and L. A. Meyers, PLoS Comput. Biol. **7**, e1002042 (2011).
[48] W. Wang, M. Tang, H. F. Zhang, and Y. C. Lai, Phys. Rev. E **92**, 012820 (2015).
[49] S. H. Strogatz, *Nonlinear Dynamics and Chaos: With Applications to Physics, Biology, Chemistry, and Engineering (Studies in Nonlinearity)*, 2nd ed. (Westview Press, Colorado, USA, 2014).
[50] P.-P. Shu, W. Wang, M. Tang, and Y.-H. Do, Chaos **25**, 063104 (2015).
[51] R. Parshani, S. V. Buldyrev, and S. Havlin, Proc. Natl. Acad. Sci. USA **108**, 1007 (2011).